Suppression of Hepatic Inflammation *via* Systemic siRNA Delivery by Membrane-Disruptive and Endosomolytic Helical Polypeptide Hybrid Nanoparticles

Hua He[†], Nan Zheng[‡], Ziyuan Song[‡], Kyung Hoon Kim[‡], Catherine Yao[‡], Rujing Zhang[‡], Chenglin Zhang[#], Yuhui Huang[#], Fatih M. Uckun[§], Jianjun Cheng[‡], Yanfeng Zhang[‖], Lichen Yin[†,*]

[†] Institute of Functional Nano & Soft Materials (FUNSOM), Jiangsu Key Laboratory for Carbon-Based Functional Materials & Devices, Soochow University, 199 Ren'ai Road, Suzhou, China, [‡]Department of Materials Science and Engineering, University of Illinois, Urbana-Champaign, 1304 W. Green Street, Urbana, IL 61801, USA, [#]The Cyrus Tang Hematology Center, the Collaborative Innovation Center of Hematology, Soochow University, China, [§]Division of Hematology-Oncology, Systems Immunobiology Laboratory, Children's Center for Cancer and Blood Diseases, Children's Hospital Los Angeles, Los Angeles, CA 90027, USA, [‖]Department of Applied Chemistry, School of Science, Xi'an Jiaotong University, Xi'an 710049, China

[*] Address correspondence to lcyin@suda.edu.cn (L. Yin)

Supporting Figures

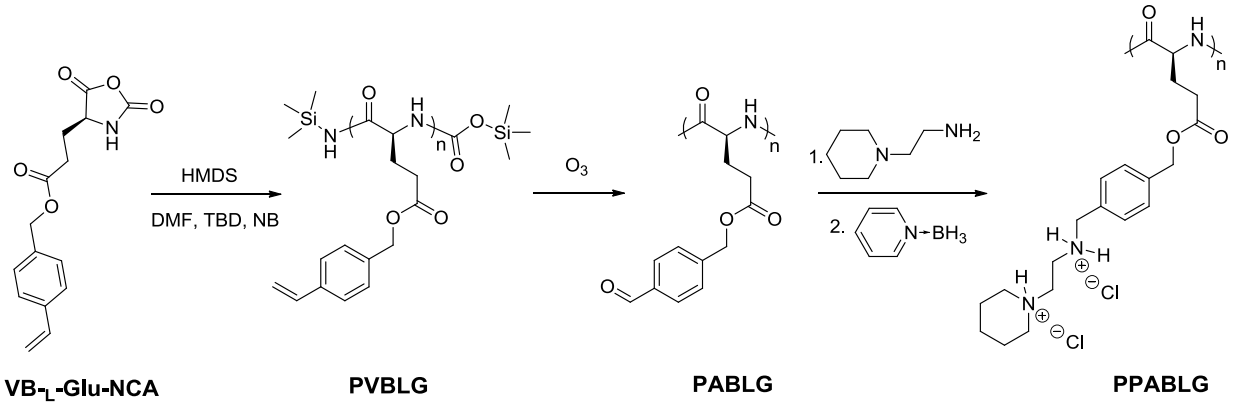

Scheme S1. Synthesis of PPABLG.

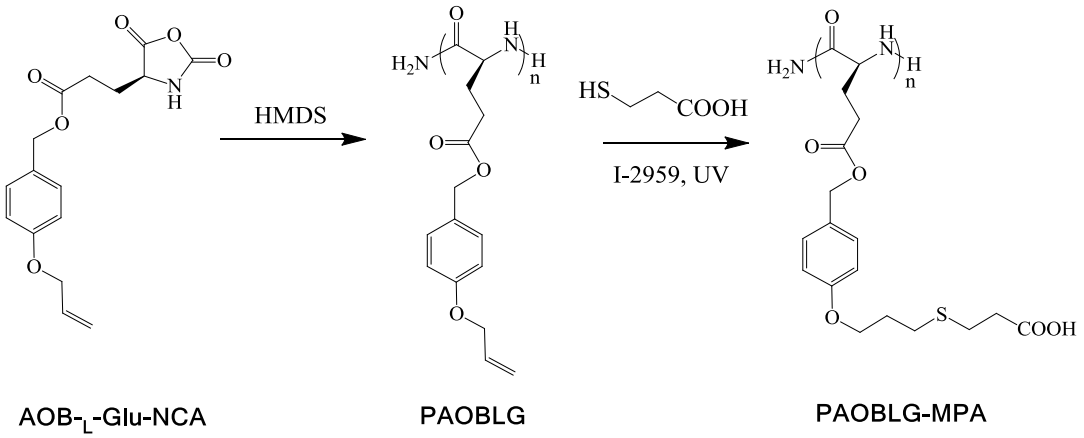

Scheme S2. Synthesis of PAOBLG-MPA.

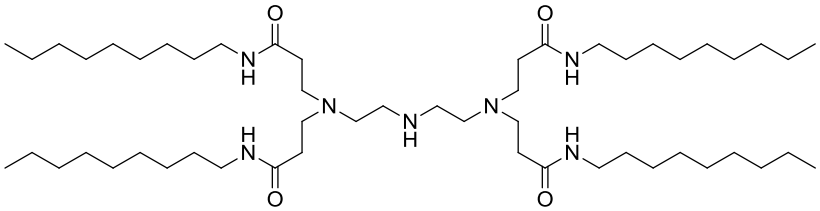

Scheme S3. Chemical structure of lipidoid.

Supplementary Table S1. Sequence of TNF-α siRNA and Scramble (Scr) siRNA

	Sequences
TNF-α sense	5'-GUCUCAGCCUCUUCUCAUUCCUGct-3'
TNF-α antisense	5'-AGCAGGAAmUGmAGmAAmGAmGGmCUmGAmGAmCmAmU-3'
Scr sense	5’-UUCUCCGAACGUGUCACGUTT-3’
Scr antisense	5’-ACGUGACACGUUCGGAGAATT-3’

Supplementary Table S2. Forward (F) and Reverse (R) TNF-α primer sequences.

Primer	Sequence
TNF-α F	CCACCACGCTCTTTCTGTCTACTG
TNF-α R	GGGCTACAGGCTTGTCACTCG

Supplementary Table S3. Leukocyte profiles of mice 2-h following i.v. administration of PPABLG HNPs (500 μg siRNA/kg) (n=4)

Group	WBC (10^9/L)	LY% (%)	MO% (%)	GR% (%)	LY (10^9/L)	MO (10^9/L)	GR (10^9/L)
Control	5.1±0.7	57.4±5.0	13.8±1.9	15.8±1.3	3.5±0.7	0.9±0.2	0.8±0.1
PPABLG HNPs	5.0±0.6	56.5±5.4	14.3±1.5	16.2±1.3	3.2±0.8	0.9±0.2	0.7±0.1

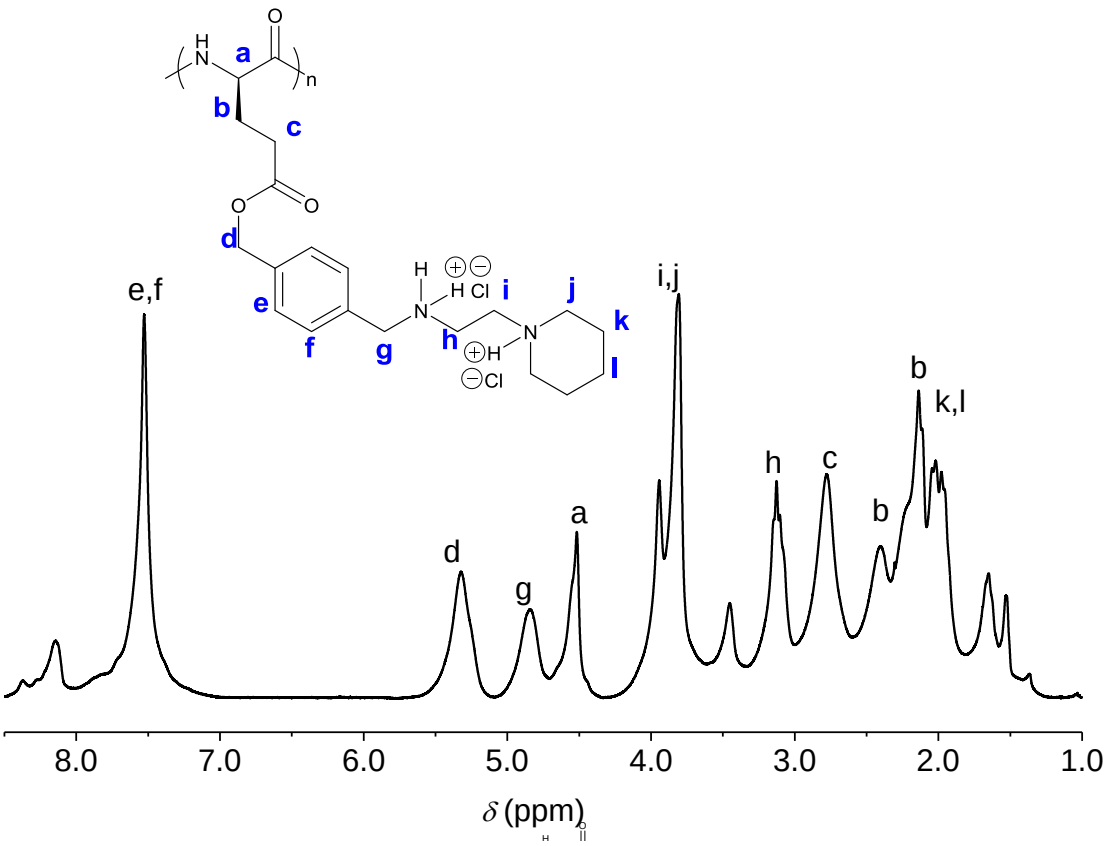

Figure S1. ^{1}H NMR spectrum of PPABLG.

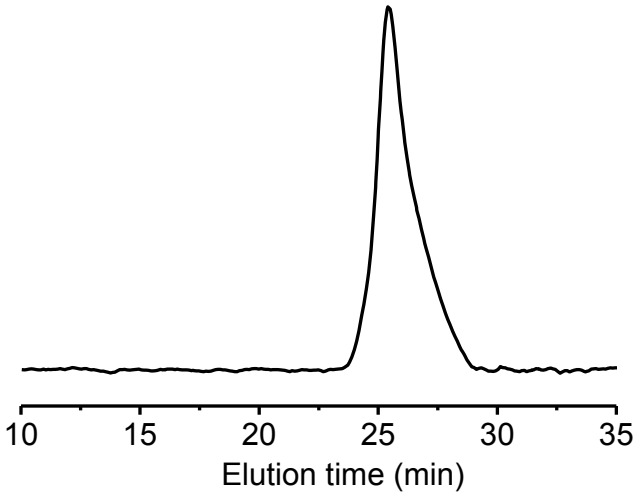

Figure S2. GPC curve of PPABLG.

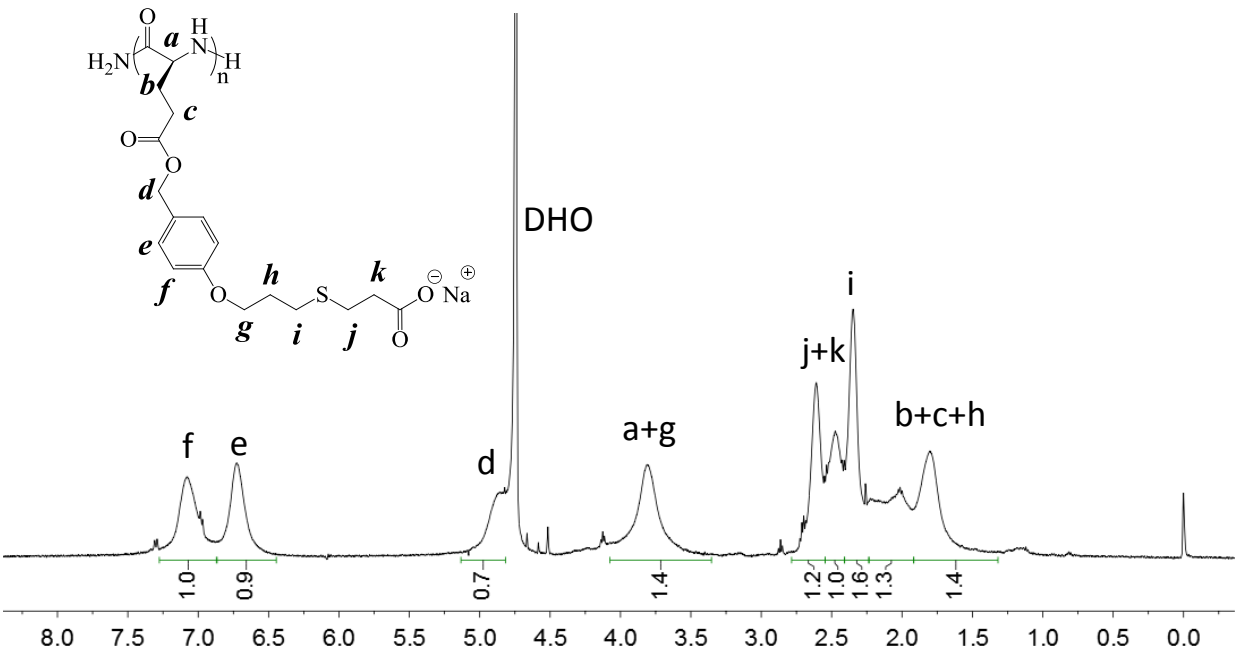

Figure S3. ^{1}H NMR spectrum of PAOBLG-MPA

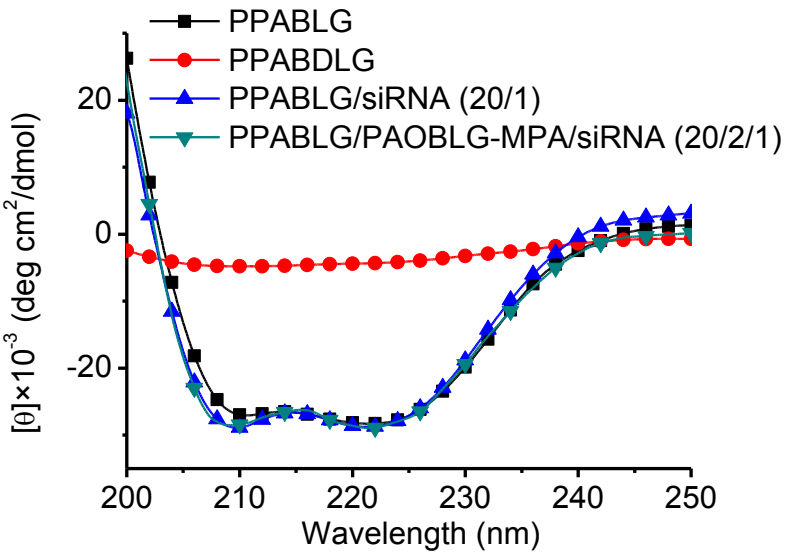

Figure S4. CD spectra of polypeptides before and after condensing siRNA.

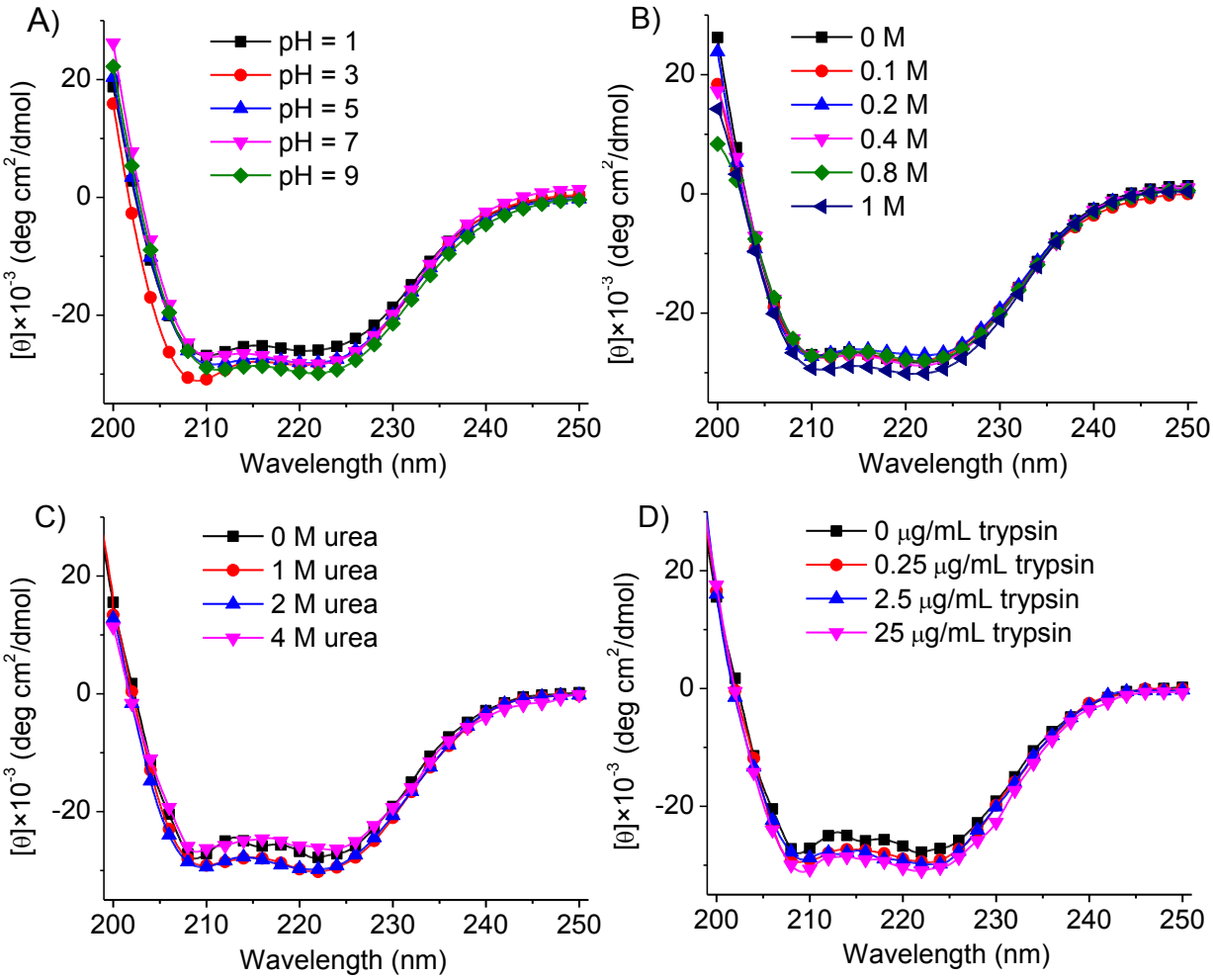

Figure S5. CD spectra of PPABLG at different pH (A), ionic strength (B), urea concentrations (C) and trypsin concentrations (treated for 2 h at 37 ℃, D).

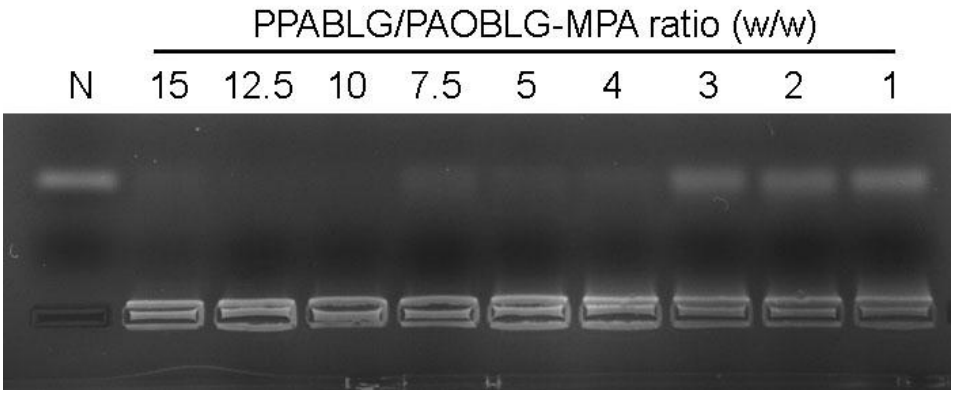

Figure S6. Condensation of TNF-α siRNA in the PPABLG/PAOBLG-MPA/siRNA hybrid nanoparticles (HNPs) at various PPABLG/PAOBLG-MPA weight ratios. PPABLG/siRNA weight ratio was maintained constant at 20:1. N represents naked siRNA.

It was observed that at lower PPABLG/PAOBLG-MPA ratios (1, 2, and 3) that referred to higher amount of negatively charged PAOBLG-MPA, siRNA cannot be fully encapsulated and a large proportion of it migrated to the anode. This result was consistent with DLS measurement that excessive amount of polyanions led to loose structures of complexes and thus siRNA cannot be compactly condensed. When the amount of PAOBLG-MPA decreased (related to higher PPABLG/PAOBLG-MPA ratio), siRNA migration was gradually retarded. At the optimal PPABLG/PAOBLG-MPA weight ratio of 10, almost all of the siRNA was retarded in the loading well, which indicated that it was completely encapsulated in the HNPs. This finding was also consistent with DLS measurement that smaller complexes of ~100 nm diameter were achieved at the PPABLG/PAOBLG-MPA weight ratio of 10.

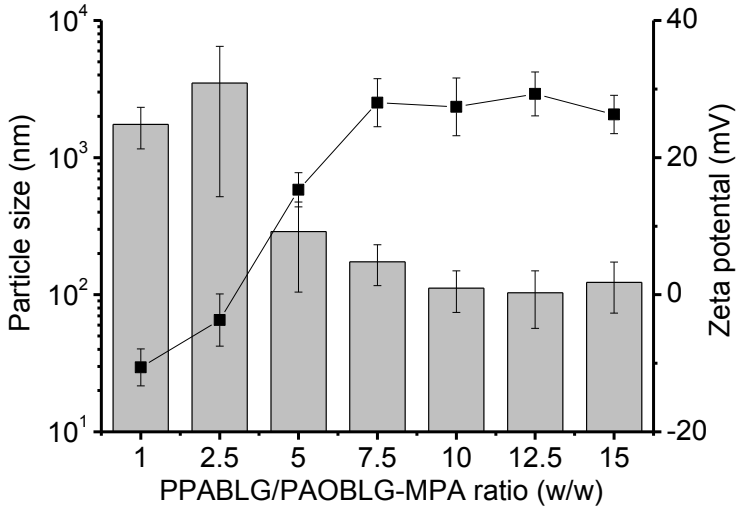

Figure S7. Size (column) and zeta potential of PPABLG/PAOBLG-MPA/siRNA hybrid nanoparticles (HNPs) at various PPABLG/PAOBLG-MPA weight ratios. PPABLG/siRNA weight ratio was maintained constant at 20:1.

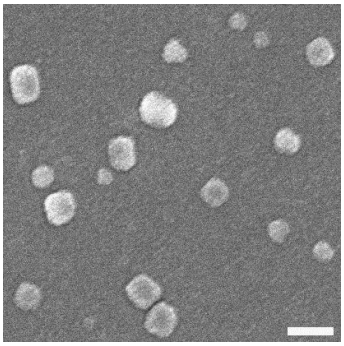

Figure S8. SEM image of PPABLG HNPs (scale bar = 200 nm).

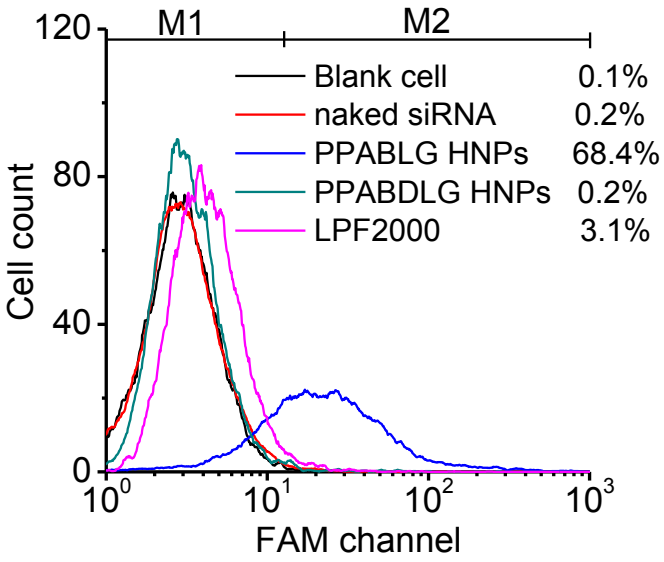

Figure S9. Flow cytometric analyses of RAW 264.7 cells after 0.5-h incubation with complexes containing FAM-siRNA under shaking (100 rpm). Non-treat cells served as the blank.

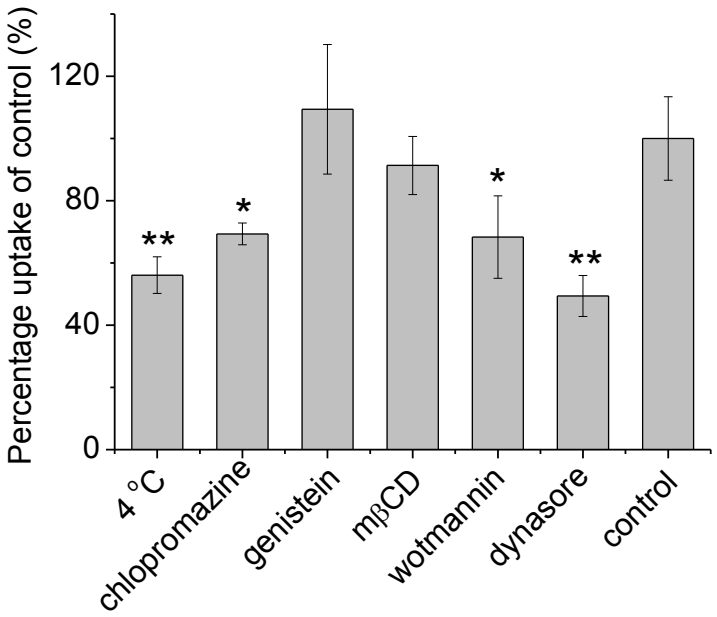

Figure S10. Mechanistic probes of the internalization pathways of PPABLG HNPs in RAW 264.7 cells by monitoring the cell uptake level of FAM-siRNA in the presence of various endocytic inhibitors (n = 3). Cells were pre-treated with inhibitors before further incubation with HNPs at 37 ℃ for 0.5 h.

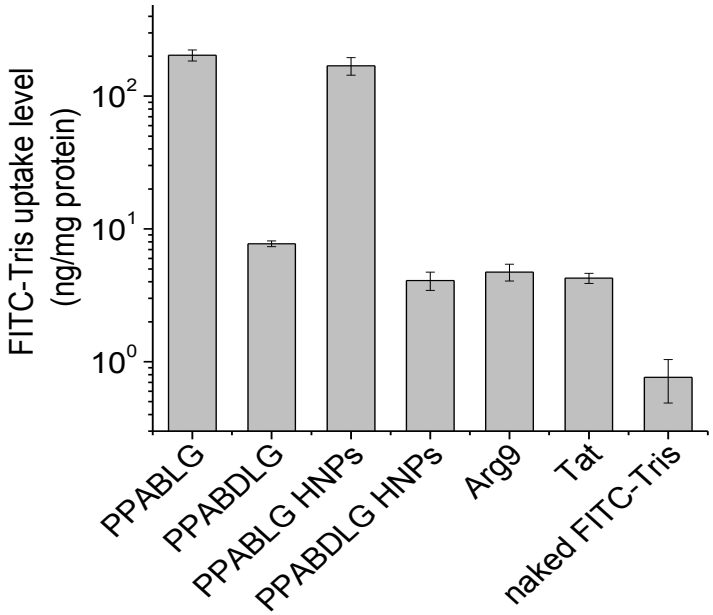

Figure S11. Uptake level of FITC-Tris in RAW 264.7 cells in the presence of free PPABLG and PPABLG HNPs following 2-h incubation at 37 ℃ (n = 3).

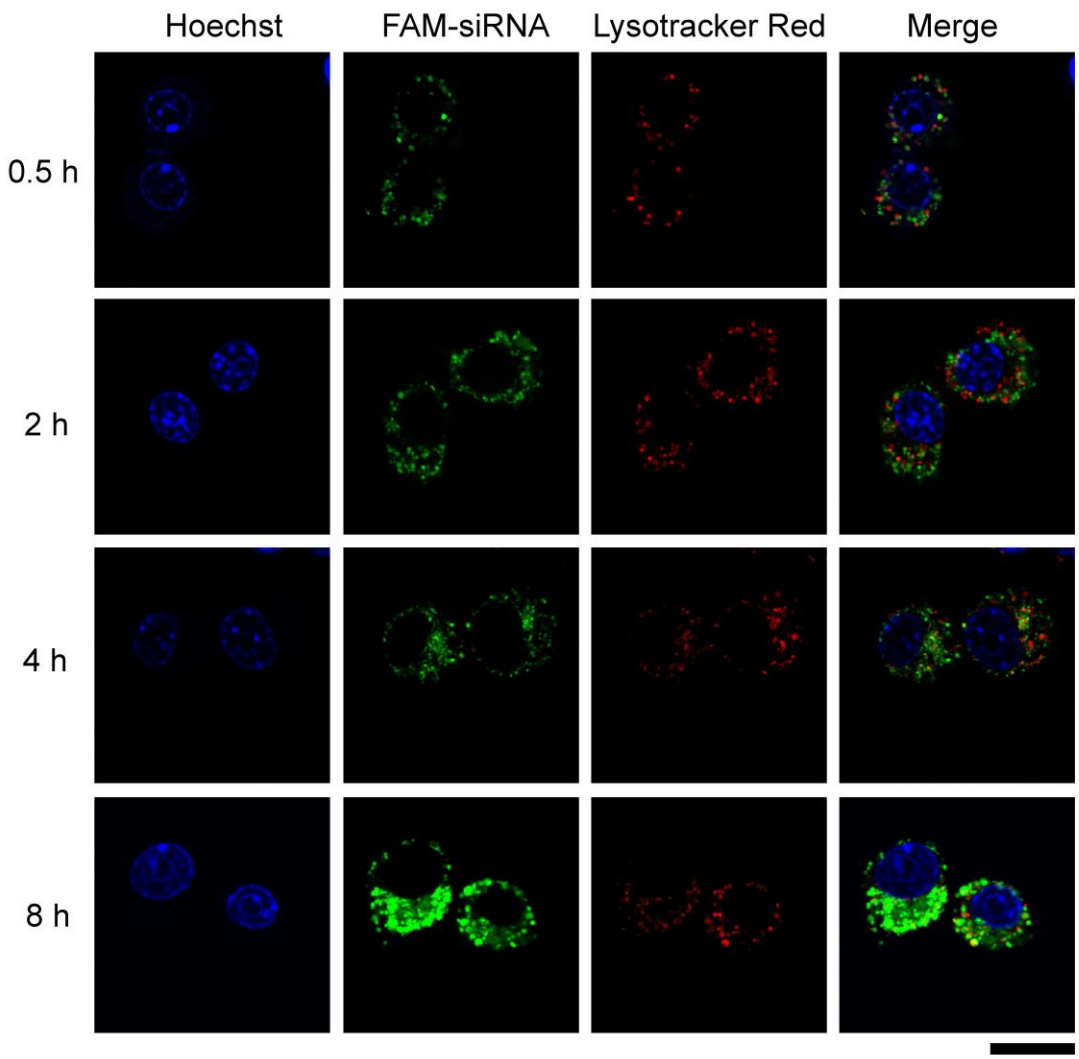

Figure S12. CLSM images of RAW 264.7 cells treated with HNPs containing FAM-siRNA for 0.5, 2, 4, and 8 h and stained with Lysotracker Red. Scale bar = 20 μm.

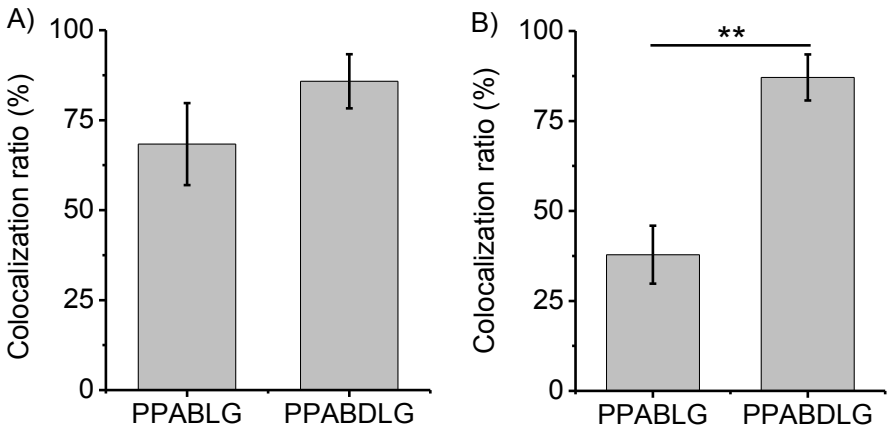

Figure S13. Colocalization ratio of FAM-siRNA with RhB-polypeptide (A) or Lysotracker Red-stained endosomes (B) from RAW 264.7 cells treated with HNPs for 4 h (n = 20).

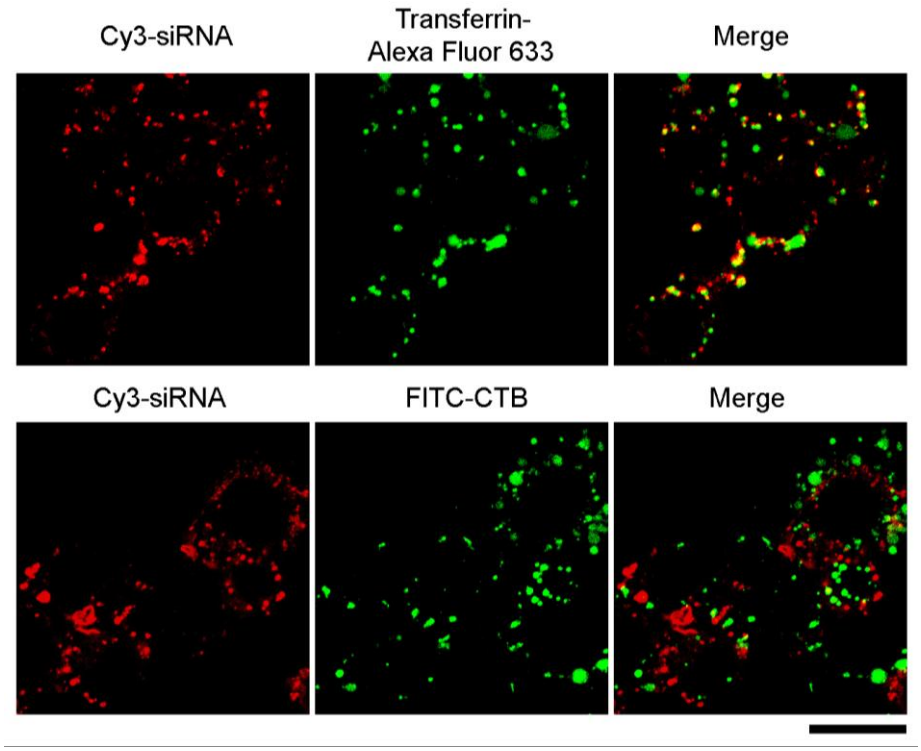

Figure S14. CLSM images of RAW 264.7 cells showing the co-localization of internalized Cy3-siRNA-containing HNPs with transferrin–Alexa Fluor 635 or FITC-CTB (bar = 20 μm).

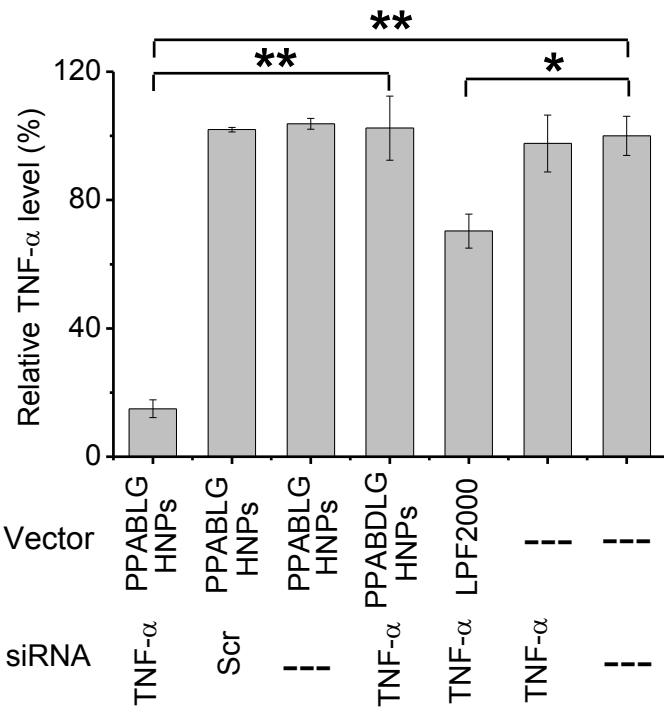

Figure S15. TNF-α level of RAW 264.7 cells following treatment with HNPs for 4 h at 0.2 μg siRNA/mL, incubation in fresh media for 20 h, and subsequent LPS stimulation at 100 ng/mL for 5 h (n = 3).

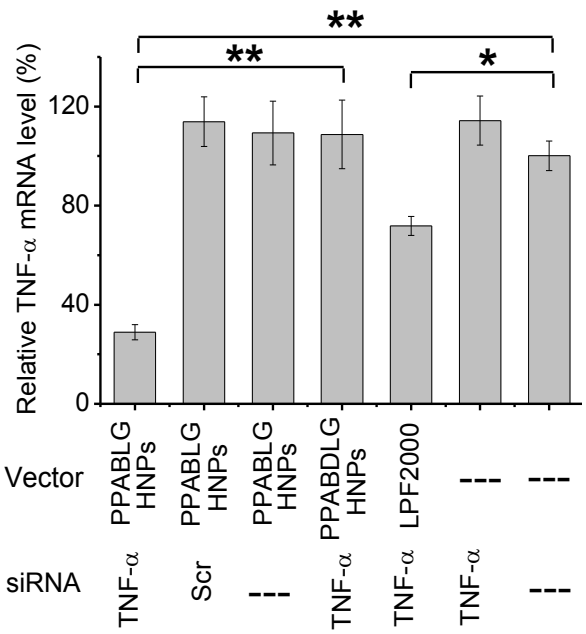

Figure S16. TNF-α mRNA level of RAW 264.7 cells following treatment with HNPs for 4 h at 0.2 μg siRNA/mL, incubation in fresh media for 20 h, and subsequent LPS stimulation at 100 ng/mL for 5 h (n = 3).

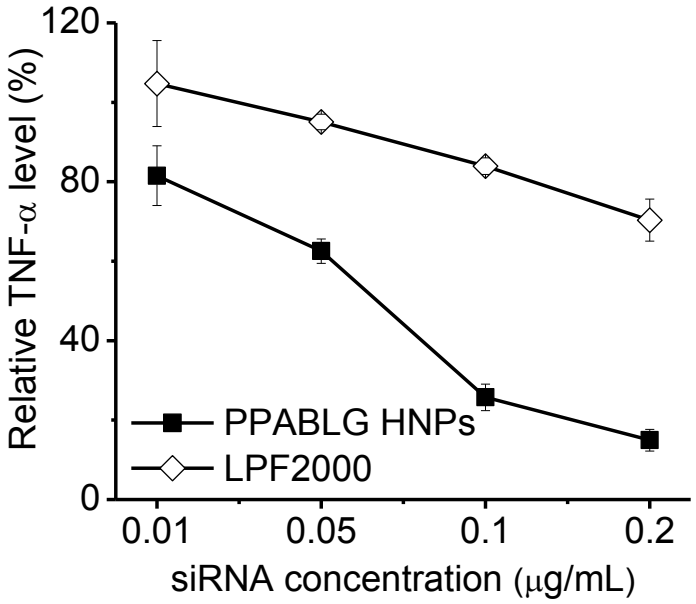

Figure S17. TNF-α levels of RAW 264.7 cells following treatment with HNPs or LPF2000/siRNA complexes at various siRNA doses (n = 3).

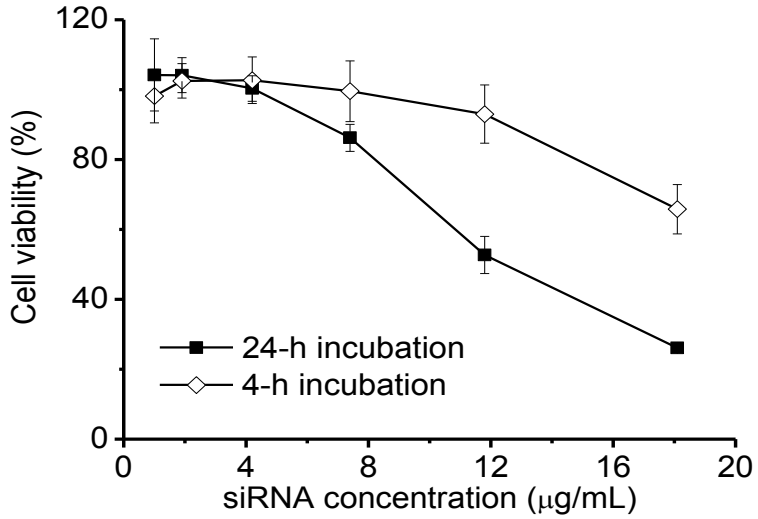

Figure S18. Cytotoxicity of HNPs towards RAW 264.7 cells at various siRNA concentrations following short-time (4 h) or long-term (24 h) incubation (n=3).

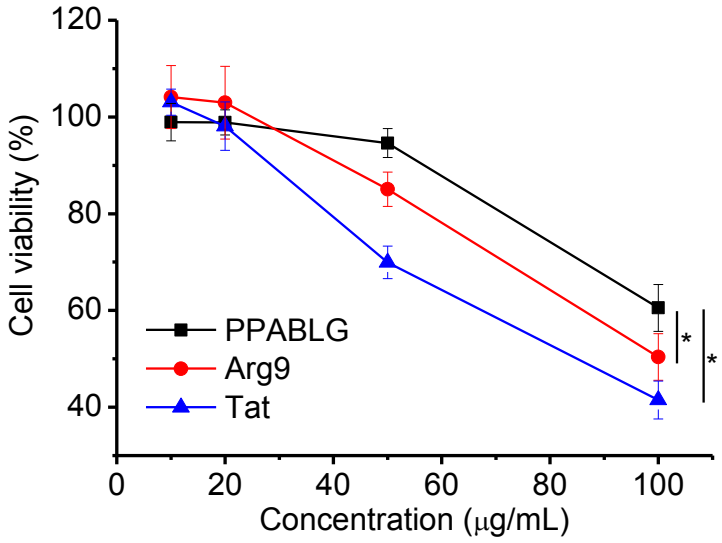

Figure S19. Cytotoxicity of PPABLG, Arg9, and Tat towards RAW 264.7 cells at various concentrations following 4-h incubation (n=3).

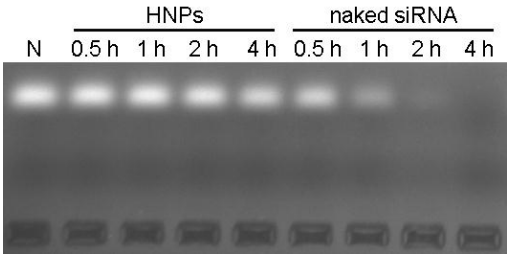

Figure S20. siRNA stability in PPABLG HNPs following treatment with mouse serum for different time.

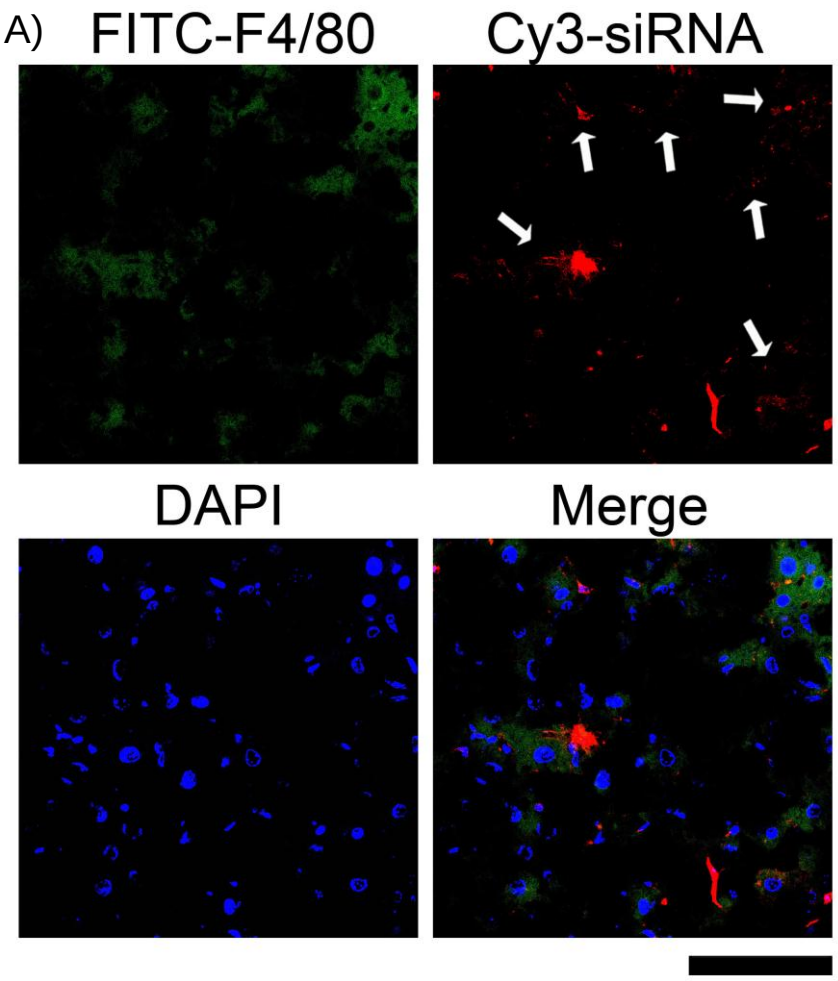
A)
FITC-F4/80
Cy3-siRNA
DAPI
Merge

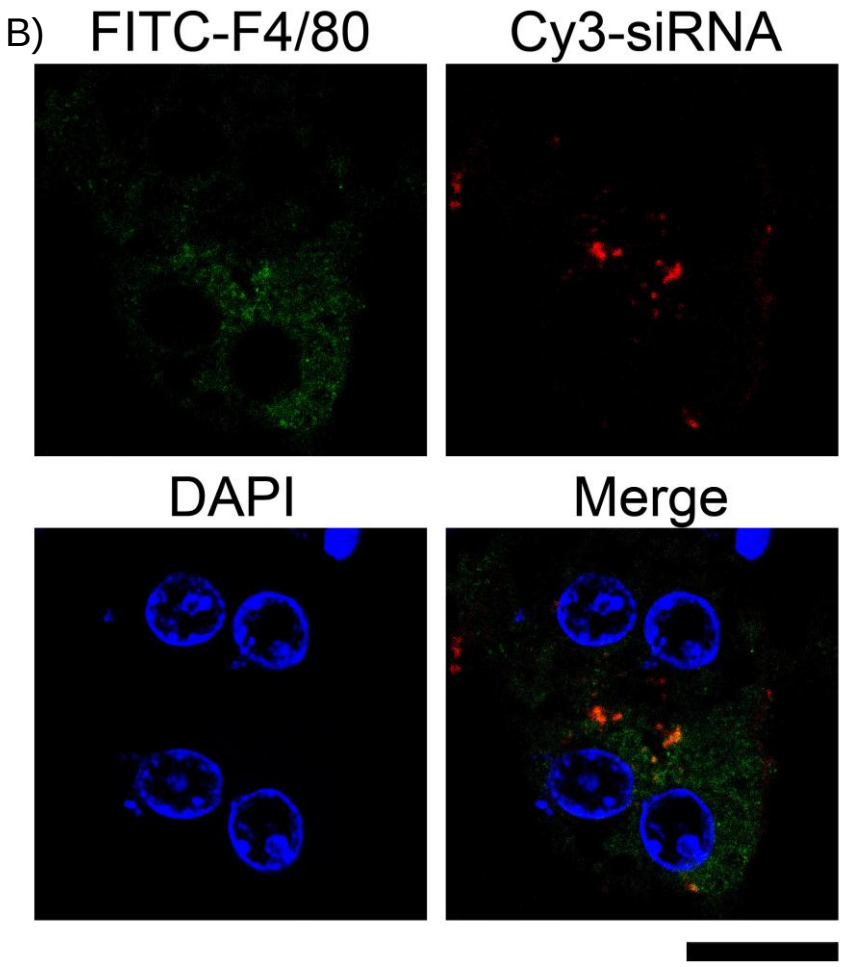

Figure S21. CLSM images of mouse liver sections stained with FITC-F4/80 (Kupffer cells) and DAPI (nuclei) 2 h after i.v. administration with Cy3-siRNA containing PPABLG HNPs at 500 μg siRNA/kg (A: large view of liver tissues; B selected view of Kupffer cells). Scale bar represents 50 μm and 20 μm in A and B, respectively. White arrows refer to Cy3-siRNA that is localized in FITC-F4/80-stained Kupffer cells.

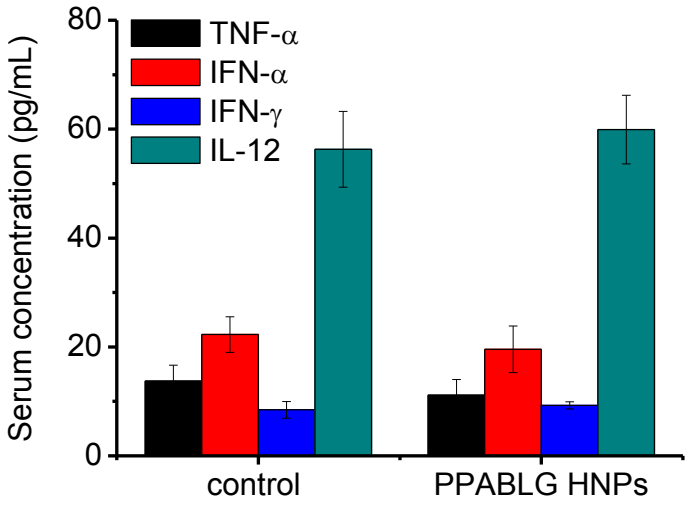

Figure S22. Serum TNF-α, IFN-α, IFN-γ, and IL-12 levels of mice 2 h after i.v. injection of PPABLG HNPs (500 μg siRNA/kg) as determined by ELISA (n = 4).

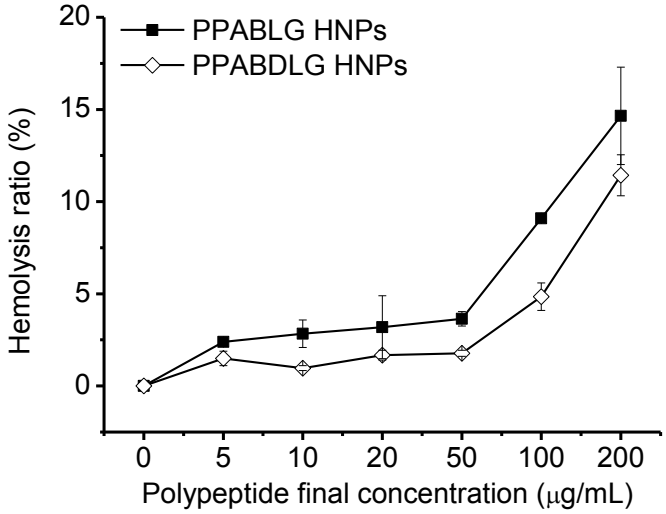

Figure S23. Hemolysis induced by PPABLG HNPs and PPABDLG HNPs (n=3).

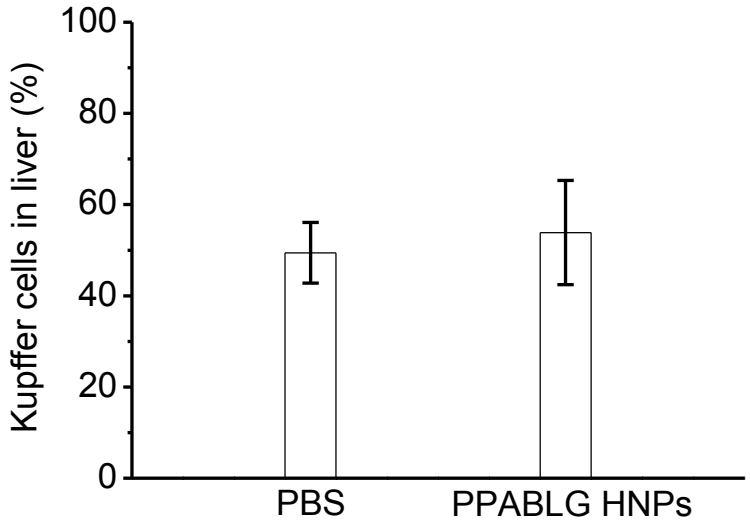

Figure S24. Percentage level of Kupffer cells in mouse liver cells determined by flow cytometry 24 h after i.v. administration of PPABLG HNPs at 500 μg siRNA/kg (n=3).

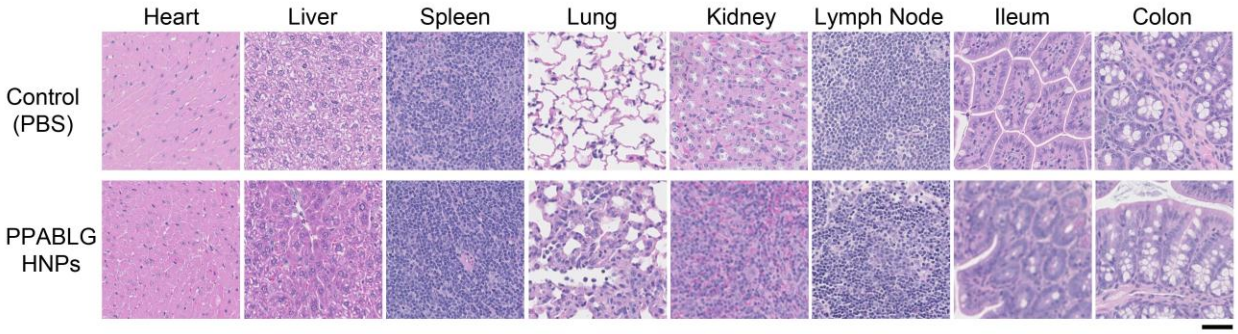

Figure S25. Histological sections of HE-stained major organs of mice 24 h post i.v. administration of PBS (control) or PPABLG HNPs (500 μg siRNA/kg). Bar represents 50 μm.